


ARTICLE

Open Access

Functional analysis of a novel C-glycosyltransferase in the orchid *Dendrobium catenatum*

Zhiyao Ren¹, Xiaoyu Ji², Zhenbin Jiao^{3,4,5}, Yingyi Luo⁶, Guo-Qiang Zhang⁵, Shengchang Tao^{1,7}, Zhouxi Lei¹, Jing Zhang¹, Yuchen Wang¹, Zhong-Jian Liu^{8,9} and Gang Wei¹ 

Abstract

Flavonoids, which are a diverse class of phytonutrients, are used by organisms to respond to nearly all abiotic stresses and are beneficial for human health. Glycosyltransferase, used during the last step of flavonoid biosynthesis, is important in flavonoid enrichment. However, little is known about glycosyltransferase in the orchid *Dendrobium catenatum* (*D. officinale*). In this study, we isolated a novel C-glycosyltransferase (designated *DcaCGT*) from the orchid *D. catenatum* by identifying and analyzing 82 putative genes in the GT1 family. *DcaCGT* could specifically catalyze not only di-C-glycosylation but also O-glycosylation. Apart from the normal function of catalyzing 2-hydroxynaringenin and phloretin to the respective di-C-glycosides, *DcaCGT* also catalyzes apigenin to cosmosiin. Targeted metabolic profiling of the substrates (2-hydroxynaringenin, phloretin, and apigenin) and products (vitexin, isovitexin, vicenin-2, nothofagin, 3',5'-di-C-glucosylphloretin, and cosmosiin) in different tissues showed that vicenin-2 was the most abundant product of this novel enzyme. Cosmosiin was detected in flowers and flower buds. We also established that *DcaCGT* functions expanded throughout the evolution of *D. catenatum*. Residual OGT activity may help *D. catenatum* resist drought stress. Our study illustrates the function, origin, and differentiation of *DcaCGT* and provides insights into glycosylation and molecular propagation processes, which can be used to improve the production of flavonoids by the cultivated medicinal plant *D. catenatum*.

Introduction

Flavonoids, a class of valuable secondary metabolites, are widely distributed in plants. More than 10,000 flavonoids and their derivatives have been identified to date¹. Flavonoid glycosides are often modified by flavonoid O- and C-glycosylation, which change the biological activities of these compounds. In plants, C-glycosylflavones protect against UV-B irradiation², exert antimicrobial effects³, and are involved in plant allelopathy⁴ and copigmentation⁵. C-glycosylflavones are critical in plant physiology and are beneficial for human health. For example, vicenin-2 is an effective flavone that shows anti-inflammatory⁶, antiglycating⁷, antispasmodic⁸, antiseptic⁹, antiplatelet,

antithrombotic¹⁰, and anticancer^{11,12} activity. Because flavonoids show such high biological activity, determining the pathways involved in the biosynthesis of flavonoid glycosides is important.

Glycosylation has an important role in modifying secondary metabolites, maintaining metabolic homeostasis, and detoxifying xenobiotics. These processes are mediated by a set of glycosyltransferases (GTs, EC 2.4.x.y). These enzymes are responsible for catalyzing glycosylation and are classified into 109 families according to the similarity of their amino-acid sequences in the Carbohydrate-Active enZYmes database (<http://www.cazy.org>). Family-1 glycosyltransferases are the largest multigene GT family, and their glycosylated products participate in the regulation of plant growth and development, such as hormone homeostasis¹³, pollination¹⁴, and interactions with the environment, such as detoxification of xenobiotics¹⁵ as well as UV tolerance¹⁶. GT1s are also called UDP-glycosyltransferases because they use

Correspondence: Zhong-Jian Liu (zjliu@fafu.edu.cn) or Gang Wei (weigang021@outlook.com)

¹School of Pharmaceutical Sciences, Guangzhou University of Chinese Medicine, Guangzhou 510006, China

²Shantou University Medical College, Shantou 515041, China

Full list of author information is available at the end of the article

These authors contributed equally: Zhiyao Ren, Xiaoyu Ji

© The Author(s) 2020



Open Access This article is licensed under a Creative Commons Attribution 4.0 International License, which permits use, sharing, adaptation, distribution and reproduction in any medium or format, as long as you give appropriate credit to the original author(s) and the source, provide a link to the Creative Commons license, and indicate if changes were made. The images or other third party material in this article are included in the article's Creative Commons license, unless indicated otherwise in a credit line to the material. If material is not included in the article's Creative Commons license and your intended use is not permitted by statutory regulation or exceeds the permitted use, you will need to obtain permission directly from the copyright holder. To view a copy of this license, visit <http://creativecommons.org/licenses/by/4.0/>.

uridine 5'-diphosphate as a sugar donor. UGTs are characterized by a highly conserved motif of a 44-amino-acid C-terminal consensus sequence called the plant secondary product glycosyltransferase (PSPG) box. Because the GT1 family has such a crucial role in the synthesis of plant secondary metabolites, members of this family have been identified mostly in model plants, crops, and fruits such as *Arabidopsis* (*Arabidopsis thaliana*)¹⁷, maize (*Zea mays*)¹⁸, wheat (*Triticum aestivum*)¹⁹, soybean (*Glycine max*)²⁰, cotton (*Gossypium* genus)²¹, peach (*Prunus persica*)²², pear (*Pyrus bretschneideri*)²³ and so on. However, little is known about the GT1 family in medicinal plants.

Dendrobium catenatum (*D. officinale*), a perennial herb in the Orchidaceae, is rich in flavonoid glycosides²⁴ and is mainly distributed in Southeast, South, and Southwest China²⁵. In the wild, *D. catenatum* largely grows year round on cliffs that receive abundant sunlight and scant water²⁶. Owing to its high medicinal value, *D. catenatum* has been widely used in traditional Chinese medicine²⁷. According to Chinese medical theory, the stems of *D. catenatum* can nourish yin, enhance gastric motility, and increase body fluids regulating immunity²⁸. Modern pharmacological studies have shown that the active ingredients of *D. catenatum* include polysaccharides²⁹, flavonoids²⁶, and bibenzyls³⁰, which promote salivation and relieve the symptoms of diabetes^{31,32}.

Glycosylation is the final step in the synthesis of flavonoid glycosides. Using oxygen, *O*-glycosyltransferases link the *O*-glycosylflavone sugar moiety to the flavonoid skeleton, whereas the glucose moiety of *C*-glycosylflavones is directly bound to the flavone backbone. *C*-glycosylflavone biosynthesis is catalyzed by *C*-glycosyltransferases (CGTs). In 2009, CGTs were first reported in rice (OsCGT)³³, followed by maize (UGT708A6)³⁴, buckwheat (FeCGTa, FeCGTb)³⁵, and soybean (UGT708D1)³⁶. Most *C*-glycosylflavones are synthesized via glucosylation of the substrate 2-hydroxyflavanone, followed by dehydrase-mediated dehydration. In 2014, another GtUF6CGT-mediated *C*-glycosylation pathway was identified in *Gentiana triflora*, showing that the sugar moiety can be directly catalyzed to the flavone skeleton³⁷. In 2017, the first CGT catalyzing the glycosylation of di-*C*-glycosides was found in citrus fruits (UGT708G1, UGT708G2)³⁸. In 2019, the first flavone 8-*C*-glycosyltransferase was discovered in *Trollius chinensis* (TcCGT)³⁹.

Di-*C*-glycosylflavones are the main flavonoids in *D. catenatum*⁴⁰. However, the amounts of secondary metabolites in *D. catenatum* vary regionally. Higher levels of di-*C*-glycosylflavones may help this plant adapt to a harsh growing environment and affect the levels of medically important ingredients. Although the last step in the formation of *C*-glycosylflavones is well characterized in plants, the gene involved in the biosynthesis of di-*C*-

glycosylflavones in *D. catenatum* has not been identified. In this study, we performed a genome-wide analysis and functional verification of CGT genes in *D. catenatum*. The levels of *DcaCGT*-related flavonoids were evaluated by ultra-high-performance liquid chromatography coupled with triple-quadrupole mass spectrometry. The haplotype distribution of *DcaCGT* was assessed in 274 samples acquired from 34 populations. Our study provides the biosynthetic pathways of di-*C/O*-glycosylflavones in *D. catenatum*, and performs a molecular phylogenetic analysis to offer insight into the evolution of the functional gene.

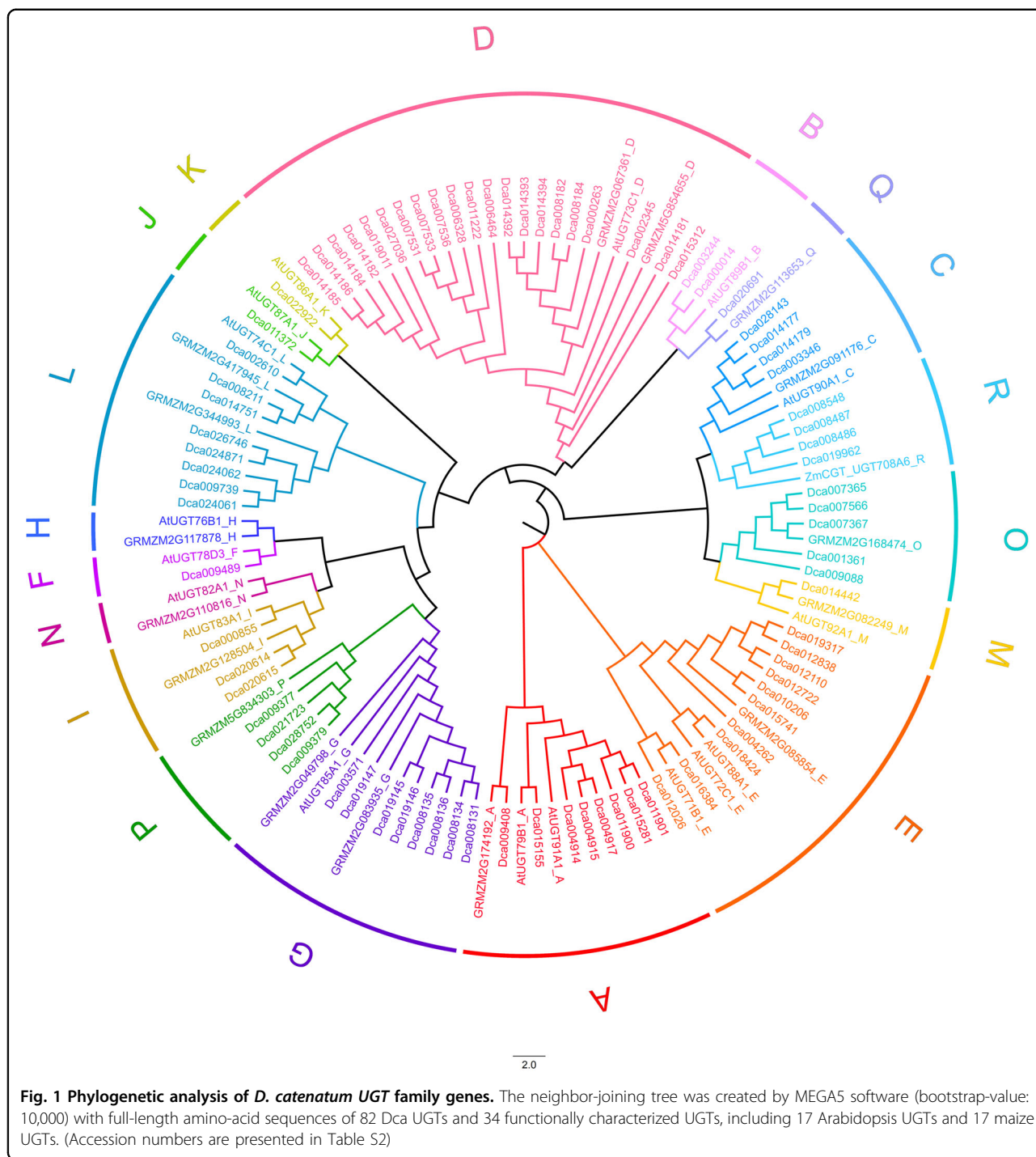
Results

Identification of UGT genes in *D. catenatum*

A BLASTP search of the *D. catenatum* genome (GenBank accession number: PRJNA262478)²⁹ was performed using the UGT-conserved PSPG box sequence as a query. A total of 82 *D. catenatum* UGTs (*E* value < 10⁻⁵) having lengths of 297–609 amino acids (with an average length of 471 amino acids) were identified. A phylogenetic tree of *D. catenatum* UGT genes was constructed by aligning the full-length amino-acid sequences of *D. catenatum* UGTs with functionally characterized plant UGTs, including *Arabidopsis* and maize UGTs (Fig. 1). These *D. catenatum* UGTs were phylogenetically divided into 16 groups, including 12 groups (A–G, I–M) that were identified in *Arabidopsis*¹⁷, 3 groups (O–Q) that were identified in maize¹⁸ and 1 group (R) that was found in seed plants⁴¹. Among the 82 listed UGTs, few were functionally characterized. The predicted molecular weight ranged from 33 to 68 kDa. The isoelectric point ranged from 4.79 to 8.9 (Table S1). Based on homology analysis, CGT gene candidates were selected from the 82 putative UGTs.

Chromosomal distribution of *D. catenatum* UGT genes

The genomic distribution of each UGT is shown in Fig. 2 to provide an overview of the location of *D. catenatum* UGT genes. The *D. catenatum* genome contained 19 chromosomes, but the 82 UGTs were distributed across only 15 chromosomes (Fig. 2). The four UGTs on the low right side of the figure are located on scaffolds and include *Dca026746*, *Dca027036*, *Dca028143*, and *Dca028752*. Different members of the UGT family were observed on each chromosome. Twenty-five UGTs were located on the longest chromosome, 01, followed by 11 members each on chromosomes 02 and 03 and 8 UGTs on chromosome 04. In addition, 1–3 UGTs were distributed on the other 11 chromosomes. Members of the same group were observed on several different chromosomes. UGTs belonging to the same group on the same chromosome tended to cluster together, whereas others were clustered separately. Groups D and E, containing the highest and second highest number of genes, respectively, were

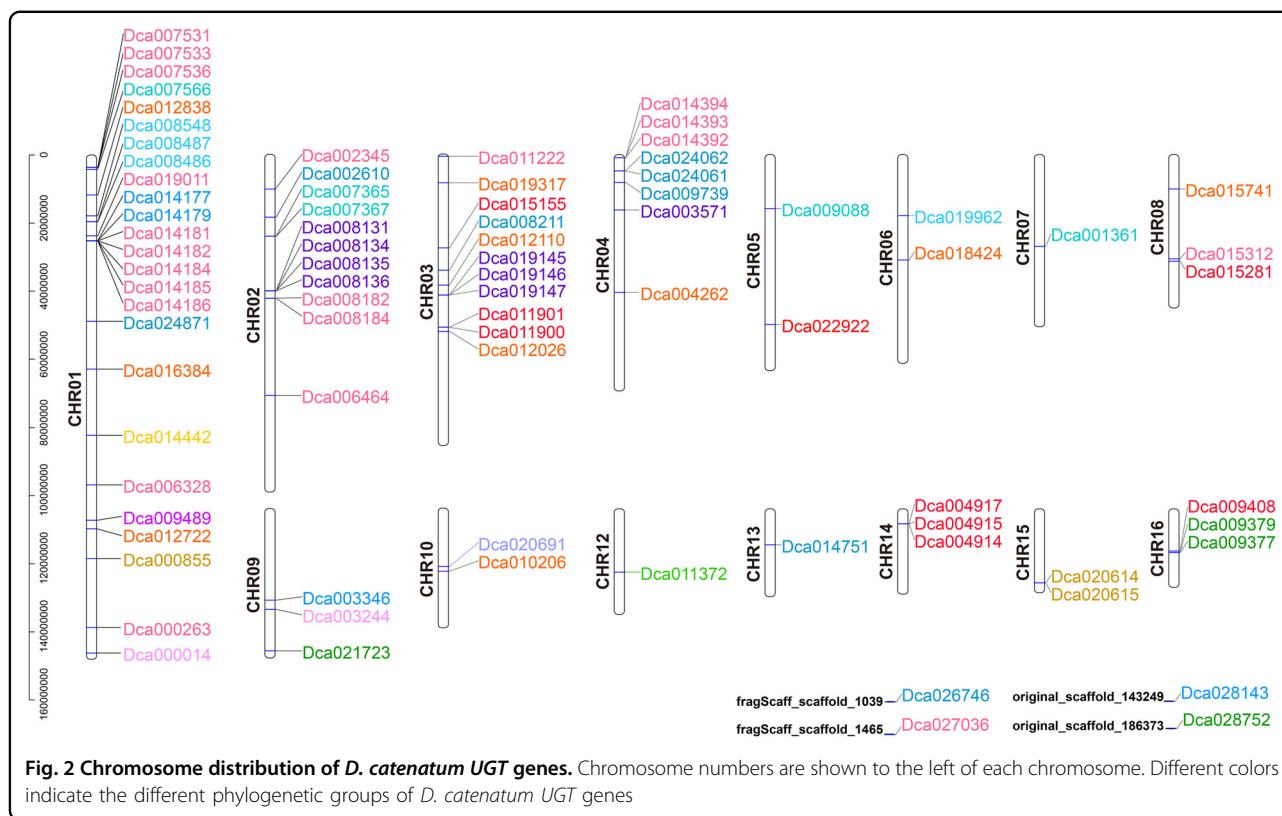


randomly distributed across five different chromosomes (Table S1).

Sequence analysis of *D. catenatum* UGT genes

Next, we analyzed exon–intron organization to investigate the evolutionary relationships within the *D. catenatum* UGT gene family. Among the 82 UGTs, 43 contained no introns, and 30 contained one intron in each

gene. For the remaining nine UGTs, seven contained two introns, and only one UGT each contained three and five introns. UGTs without introns occurred more commonly than those with introns. For the UGT groups, 100% intron loss was observed in genes of groups B, C, and Q, followed by 76% of genes in group D and 60% of genes in group M. Conversely, all genes in groups F, G, H, I, and J contained introns. A total of seven (87%) UGTs in group G



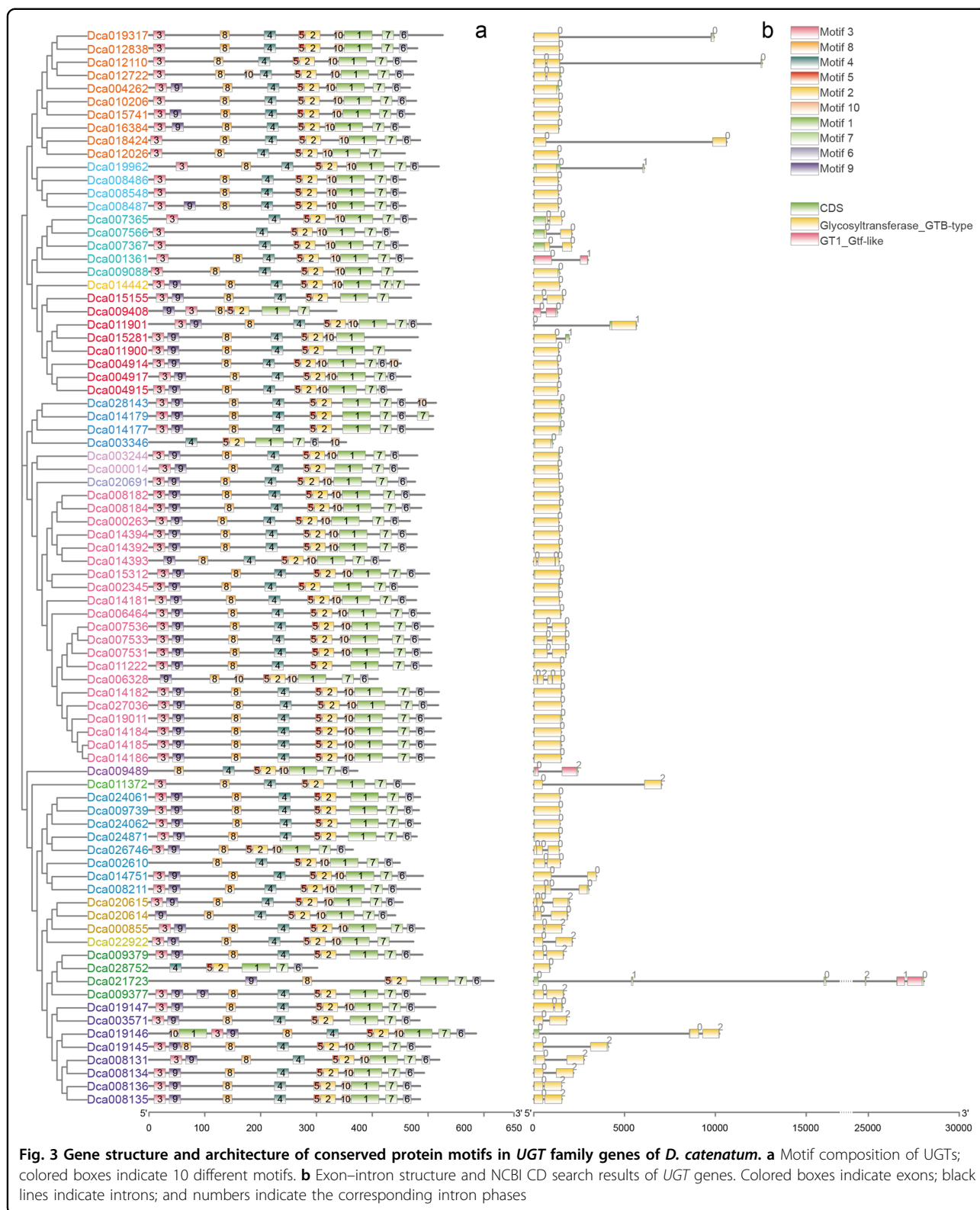
contained one intron. These positions of intron insertion were determined to be highly conserved after mapping the introns via alignment of amino-acid sequences. Intron-insertion positions varied in groups A, E, O, and R. Among the 52 total introns detected in *D. catenatum* UGT sequences, 48, 2, and 2 were in phases 0, 1, and 2, respectively. In addition, 92% of introns were in phase 0, which is far greater than the number in phases 1 and 2. Based on the information presented above, introns in *D. catenatum* family-1 UDP-glycosyltransferase clusters were deemed to not be completely conserved. In addition, an NCBI CD search showed that most of the 82 UGTs were GTB-type glycosyltransferases (Fig. 3b).

A schematic representation of the structure of all *D. catenatum* UGT proteins was constructed from the results of MEME motif analysis. As shown in Fig. 3a, motifs 1, 2, and 5 were widely distributed in every gene. Motif 1 was the location of the PSPG box, whereas the protein architecture of motifs 2 and 5 was speculated to be conserved in *D. catenatum* UGTs. Members within the same groups were usually found to share similar structures. For example, all members in group O, three of four genes in group R and 7 of 10 genes in group E showed the absence of motif 9. Three-fifths of the UGTs in group O showed the loss of motif 8. Together with the results of the phylogenetic analysis, this similarity in motif arrangements among *D. catenatum* UGT proteins within

subgroups indicates that the subfamily classification of UGTs may be based on partially conserved protein domains.

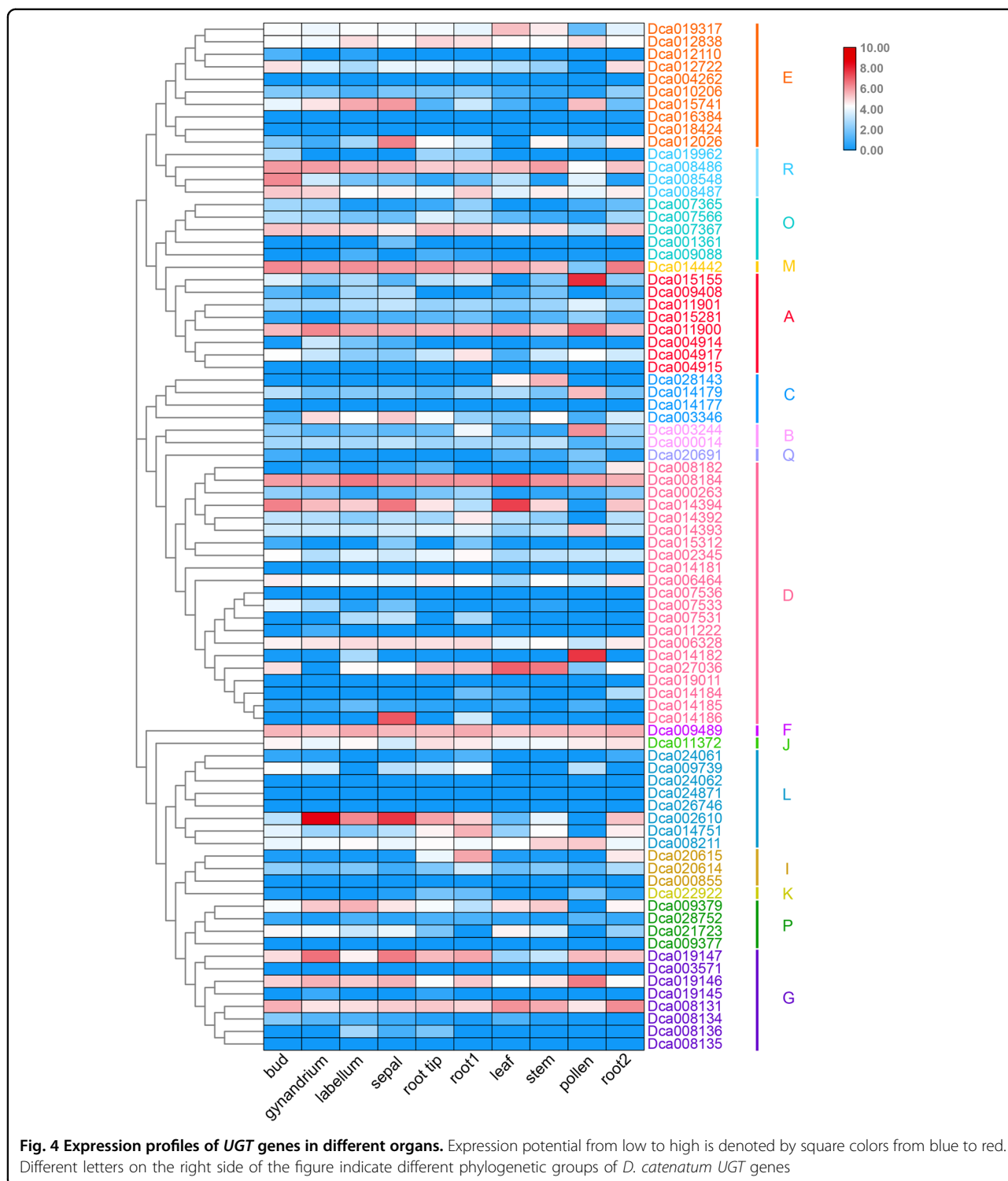
Gene expression analysis of different organs of *D. catenatum*

The transcriptome revealed 82 UGTs with varied expression patterns across 10 plant tissues (Fig. 4), including the bud, gynandrium, labellum, sepal, root tip, day root (root1), leaf, stem, pollen, and night root (root2) (GenBank accession number: PRJNA348403)⁴². Sixty-nine UGT genes were expressed in at least two organs, whereas transcription of 13 UGTs was not observed. For the unexpressed UGTs, three genes were located in groups D and L, two genes were located in group E, and the other six genes were distributed among groups A, C, G, I, and P. We examined the possible expression pattern of UGTs in different tissues and found that 58 UGTs were expressed in the bud and sepal, which were the organs showing the highest number of expressed UGTs. The lowest number of UGTs (49) was found in pollen tissue. The number of UGTs expressed in other organs, such as the gynandrium, labellum, root tip, day root, leaf, stem, and night root, ranged between 49 and 58. We also observed that unexpressed genes in these tissues were mostly distributed in groups D, G, L, and E. In contrast to 35 UGTs, which were expressed in all nine plant tissue samples, nine UGTs were



expressed in all but one organ sample. *Dca027036* and *Dca015281* expression was not detected in the gynandrium, that of *Dca015155* and *Dca012026* was not

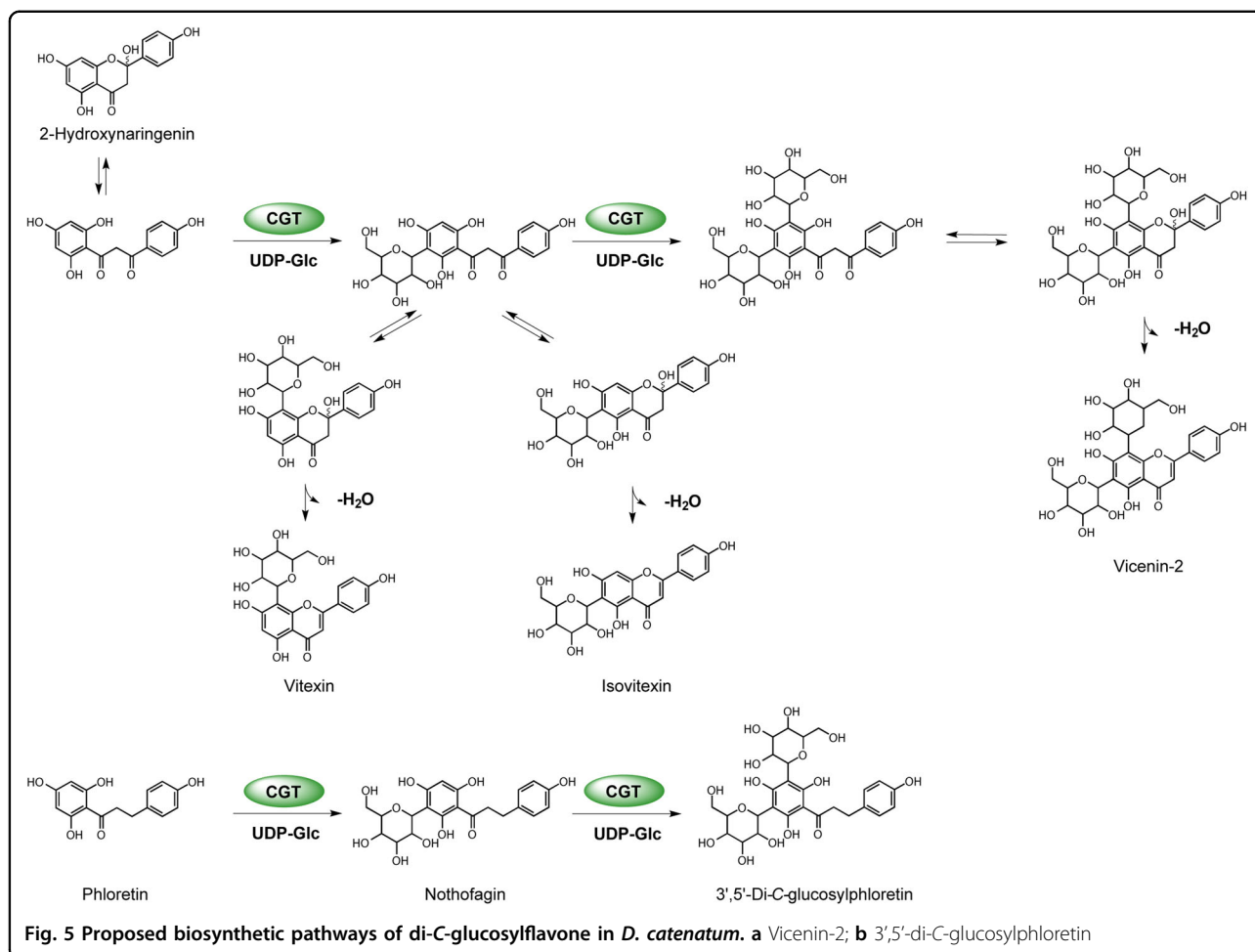
detected in leaves, that of *Dca009379*, *Dca014392*, *Dca012722*, and *Dca002610* was not detected in pollen, and that of *Dca008134* was not detected in the night root.



These results suggest that high transcription levels of a specific UGT may lead to increased levels of related components, whereas unexpressed UGTs in different organs may result in the absence of certain components in these organs.

Properties of recombinant *D. catenatum* CGT expressed in *E. coli* and in vitro enzymatic activity assays

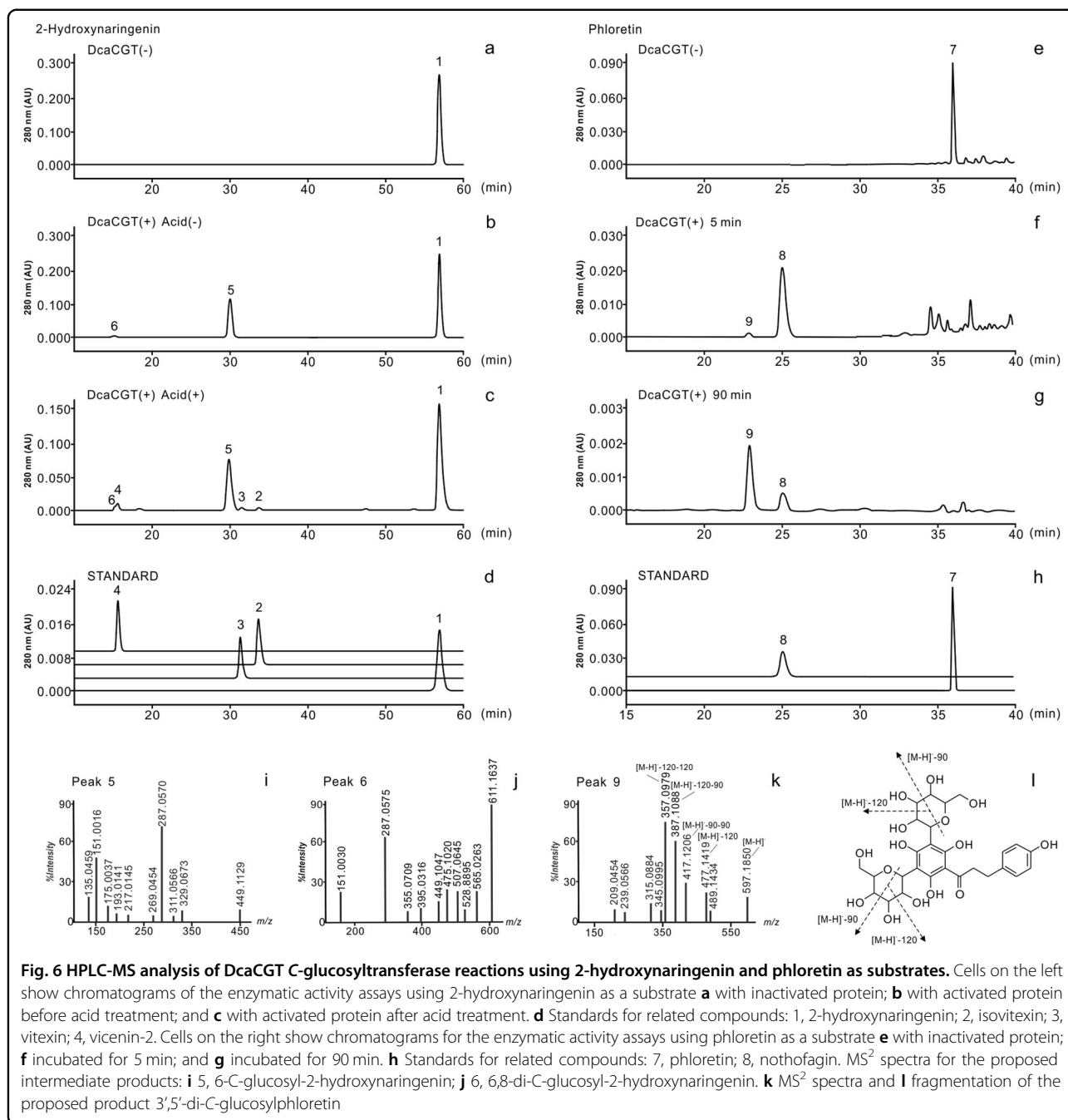
To determine the functions of *DcaCGT*, full-length cDNA was obtained from *D. catenatum*. The CDS region was cloned into a pET32a(+) vector and transformed into



Escherichia coli Rosetta (DE3) to investigate the catalytic activity of the enzyme encoded by the isolated putative *DcaCGT* gene (GenBank accession number: MT452646). The expressed recombinant proteins contained a fused His6 tag and showed a molecular weight of 66.1 kDa when analyzed via SDS-PAGE (Fig. S1). Enzymatic activity assays were conducted using three flavanone substrates: 2-hydroxynaringenin, phloretin, and apigenin. Glycoside products were analyzed by liquid chromatography–mass spectrometry (LC-MS).

The resulting recombinant protein *DcaCGT* displayed C-glycosylation activity against 2-hydroxynaringenin, indicating that it was a CGT derived from *D. catenatum* plants. The typical reaction pattern catalyzed by *DcaCGT* is shown in Fig. 5. When 2-hydroxynaringenin was used as the substrate, it was converted into 6-C-glucosyl-2-hydroxynaringenin at m/z 449 (peak 5) and 6,8-di-C-glucosyl-2-hydroxynaringenin at m/z 611 (peak 6); these were the main products following the enzymatic reaction (Fig. 6). After treatment with HCl, these compounds were dehydrated. Two products of

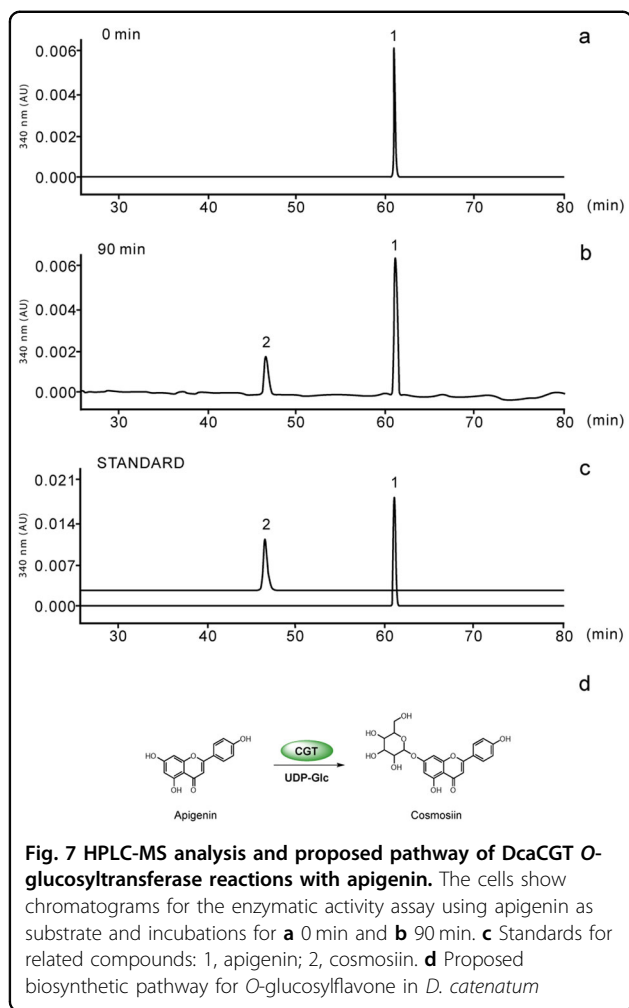
dehydrated derivatives (peaks 2 and 3) showed C-glycoside moiety fragment ions of $[M-H-90]^-$ and $[M-H-120]^-$ ⁴³, which corresponded to vitexin (m/z 431) and isovitexin (m/z 431), respectively. Vitexin and isovitexin levels decreased as the reaction continued, whereas the level of vicenin-2 (m/z 593) increased (Fig. S2). All the dehydrated products showed the same retention time and fragmentation pattern as those of the respective standards⁴⁴. Moreover, two products were observed when phloretin was used as the substrate. The MS² spectrum of peak 8 at m/z 345 $[M-H-90]^-$ and 315 $[M-H-120]^-$ showed the presence of nothofagin⁴⁵. Peak 9 showed a pseudomolecular ion at m/z 597. The fragments at m/z 477 $[M-H-120]^-$, 417 $[M-H-90-90]^-$, and 357 $[M-H-120-120]^-$ suggested that most of these were gained from the loss of sugar residues (Fig. S3). Based on ESI-MS data, this product was identified as 3',5'-di-C-glucosylphloretin⁴⁶. These results indicate that *DcaCGT* encodes a glycosyltransferase that catalyzes the conversion of flavanones to flavonoid di-C-glucoside via flavonoid mono-C-glucoside intermediates.



In addition, when we used apigenin as a substrate, a new product was detected by LC-MS (Fig. 7). MS analysis showed a precursor at m/z 431 (Fig. S4). The fragments at m/z $[M-H-162]^-$ indicated apigenin bonding to glucose via *O*-linkage⁴⁷. The new product exhibited the same retention time and mass fragmentation pattern as those of the authentic standard for cosmosiin. Hence, these results support those obtained using bioconversion assays and indicate that DcaCGT can catalyze substrates to not only di-C-glycosylflavone but also *O*-glycosylflavone.

Flavonoids of *D. catenatum*

The biosynthesis of flavones (vitexin, isovitexin, vicenin-2, nothofagin, 3',5'-di-C-glycosylphloretin, and cosmosiin) from flavanones (2-hydroxynaringenin, phloretin, and apigenin) is catalyzed by UDP-glycosyltransferases. To explore the distribution of UGT-related flavanones and flavone glycosides accumulated in *D. catenatum*, we prepared methanolic extracts from flower buds, flowers, leaves, stems, and roots for UPLC-MS analysis. The chromatogram and mass spectrometry conditions of the



eight investigated compounds as well as the internal standard are shown in Fig. S5 and Table S4. Among the nine targeted flavonoids, eight compounds (except 3',5'-di-C-glucosylphloretin) were found in the different organs. The compositions of these compounds varied among the organs (Fig. S6). C-glycosylflavone accumulation was significantly higher than that of O-glycosylflavones in the plant tissues examined in this study. Vicenin-2 and its intermediate products were more abundant than nothofagin and its intermediate products. 2-Hydroxynaringenin, phloretin, and apigenin were mostly detected in the roots, stems, and leaves, while vicenin-2, vitexin, isovitexin, nothofagin, and cosmosiin showed higher levels in flowers and flower buds. Flower buds showed the greatest variety of flavone glycosides and included vitexin, isovitexin, and vicenin-2, whereas roots had the lowest levels of vicenin-2 and intermediate products. These results, together with those of transcriptomic analysis, indicate that DcaUGT may mainly be used to biosynthesize vicenin-2 and that higher levels of vicenin-2 may be related to higher *DcaUGT* transcript levels in *D.*

catenatum. Other substrates and products, such as apigenin and cosmosiin, were not detected simultaneously in the same organ. This may be related to different periods of gene expression and harvest times (Fig. 8 and Table 1).

Molecular phylogenetic analysis of *D. catenatum* CGTs

A neighbor-joining tree was constructed based on the deduced amino-acid sequences of the seven clusters (Fig. 9) and included flavone 7-OH glycosylation (cluster 1), flavonoid glycoside sugar-O-sugar links (cluster 2), 3-OH glycosylation (cluster 3), 5-OH glycosylation (cluster 4), isoflavone 7-OH glycosylation (cluster 5), plant CGTs (cluster 6), and bacterial CGTs (cluster 7). Detailed information on these UGTs is summarized in Table S5. DcaCGT is listed in cluster 6 with other plant CGTs, indicating that they may have evolved from the same ancestral gene. DcaCGT and ZmCGT were grouped into a clade, suggesting that they may have similar active sites used to catalyze flavonoid C-glycosides and O-glycosides simultaneously. Alignments of the amino-acid sequences of DcaCGT and other plant C-glycosyltransferases are shown in Fig. S7.

Multiple sequence alignment analysis of *DcaCGT* from *D. catenatum* collected from different geographical locales

To examine the evolutionary origin of *DcaCGT*, full-length *DcaCGT* was extracted and analyzed from 279 accessions of *Dendrobium*, including resequencing data from 274 *D. catenatum* samples obtained from 34 populations and data from five samples of *D. huoshanense* obtained from a single population. As many as 132 haplotypes were observed among the aligned sequence data from the 274 *D. catenatum* samples. The *D. huoshanense* population was chosen as the root. Phylogenetic analysis indicated that *DcaCGT* haplotypes were grouped mainly into three clusters: the ancestral Cluster_a and evolutionary clade Clusters_b and _c, with 100 and 9.8% bootstrap support, respectively (Fig. 10a). In addition, the 274 samples were unevenly distributed among the three clades, with Cluster_a containing 46 samples (32 haplotypes), Cluster_b containing 72 samples (36 haplotypes), and Cluster_c containing 156 samples (64 haplotypes). A comparison of nucleotide diversity among these three clusters indicated that Cluster_a ($\theta = 0.00752$; $\pi = 0.00461$) exhibited higher diversity than Cluster_b ($\theta = 0.00576$; $\pi = 0.00244$) and Cluster_c ($\theta = 0.00705$; $\pi = 0.00287$). Negative Tajima's *D* values were observed among these clades. However, significant negative Tajima's *D* values were only observed in the evolutionary clades for Cluster_b and Cluster_c. *DcaCGT*, the CGT identified in this study, was grouped in Cluster_c. These results suggest that natural selection acted on the evolutionary clades. Significant differentiation was found among Cluster_a, Cluster_b, and Cluster_c because

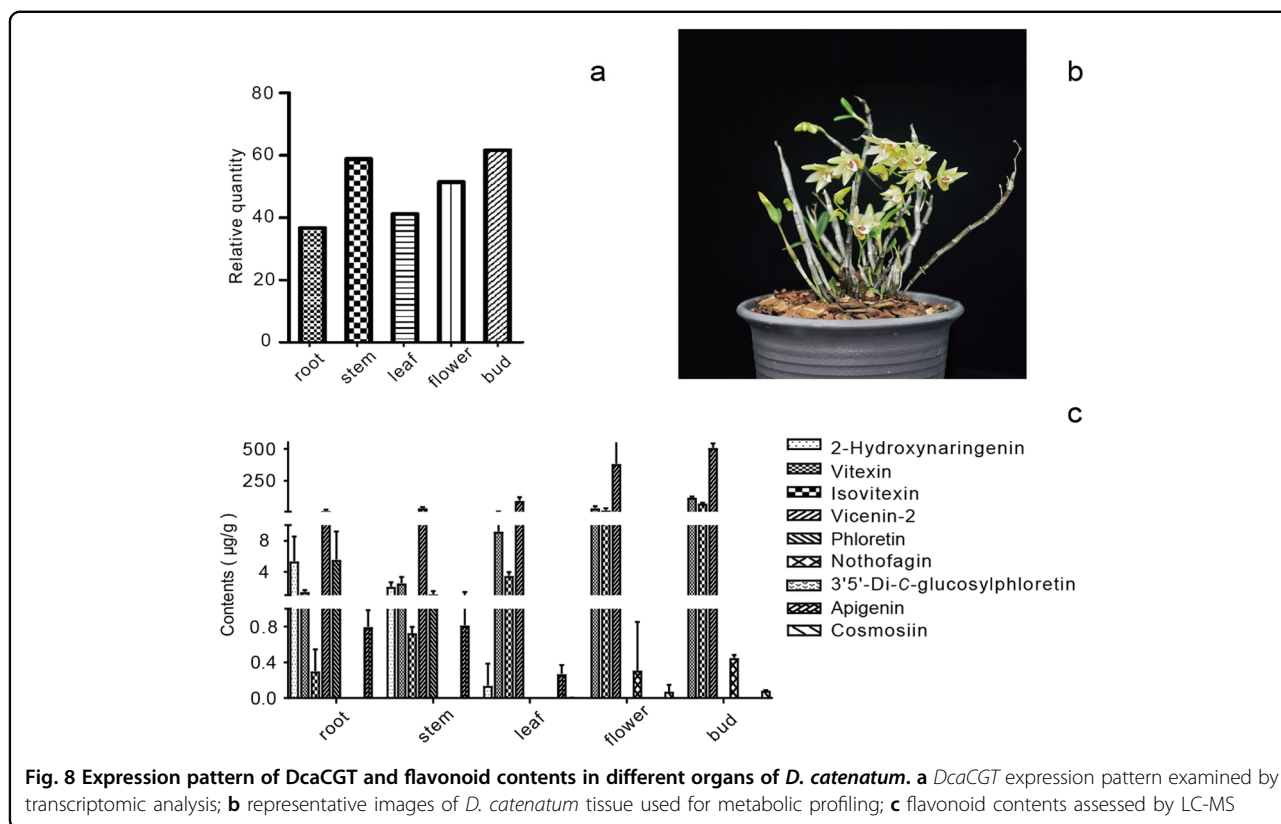


Table 1 Flavonoids in different organs of *D. catenatum*

Name	RT (min)	Formula	Parent/product ion	Flavonoid contents ($\bar{x} \pm s$, $\mu\text{g/g}$, $n = 3$)				
				Root	Srem	Leaf	Flower	Flower bud
2-Hydroxynaringenin	8.59	C ₁₅ H ₁₂ O ₆	286.97/151.00	5.39 ± 3.17	2.11 ± 0.56	0.14 ± 0.24	n.d.	n.d.
Vitexin	5.81	C ₂₁ H ₂₀ O ₁₀	430.95/311.00	1.46 ± 0.20	2.55 ± 0.80	9.21 ± 2.17	38.88 ± 13.69	121.19 ± 6.95
Isovitexin	6.03	C ₂₁ H ₂₀ O ₁₀	430.88/311.00	0.30 ± 0.24	0.73 ± 0.07	3.53 ± 0.45	21.36 ± 15.36	74.65 ± 4.93
Vicenin-2	3.64	C ₂₇ H ₃₀ O ₁₅	592.99/352.90	16.90 ± 8.34	38.61 ± 6.97	95.74 ± 28.07	383.52 ± 187.65	507.95 ± 35.24
Phloretin	9.12	C ₁₅ H ₁₄ O ₅	273.740/167.80	5.59 ± 3.60	1.15 ± 0.39	n.d.	n.d.	n.d.
Nothofagin	6.80	C ₂₁ H ₂₄ O ₁₀	435.09/314.90	n.d.	n.d.	n.d.	0.31 ± 0.62	0.45 ± 0.03
Apigenin	9.26	C ₁₅ H ₁₀ O ₅	268.76/117.10	0.80 ± 0.19	0.82 ± 0.61	0.27 ± 0.10	n.d.	n.d.
Cosmosiin	7.58	C ₂₁ H ₂₀ O ₁₀	430.76/268.00	n.d.	n.d.	n.d.	0.08 ± 0.08	0.09 ± 0.00

n.d. not detected.

population pairwise *Fst* values among these clusters were higher than 0.25⁴⁸. There was a greater degree of differentiation between Cluster_a and Cluster_c, with an *Fst*-value of 0.58246 ($P < 0.001$), than between the other pairs of clusters. The differentiation between Cluster_a and Cluster_b and that between Cluster_b and Cluster_c were similar, with *Fst* values of 0.46405 ($P < 0.001$) and 0.47014 ($P < 0.001$), respectively.

Geographically, we found that the original Cluster_a was distributed only among 20 populations, mainly from Southwest, North, and easternmost China. Cluster_b covered 26 populations distributed in eastern and middle portions of China. Cluster_c, the newest evolutionary clade, contained all the populations except Xiushui, Jiangxi. Most populations in western China occupied a large proportion of Cluster_c (Fig. 10b).

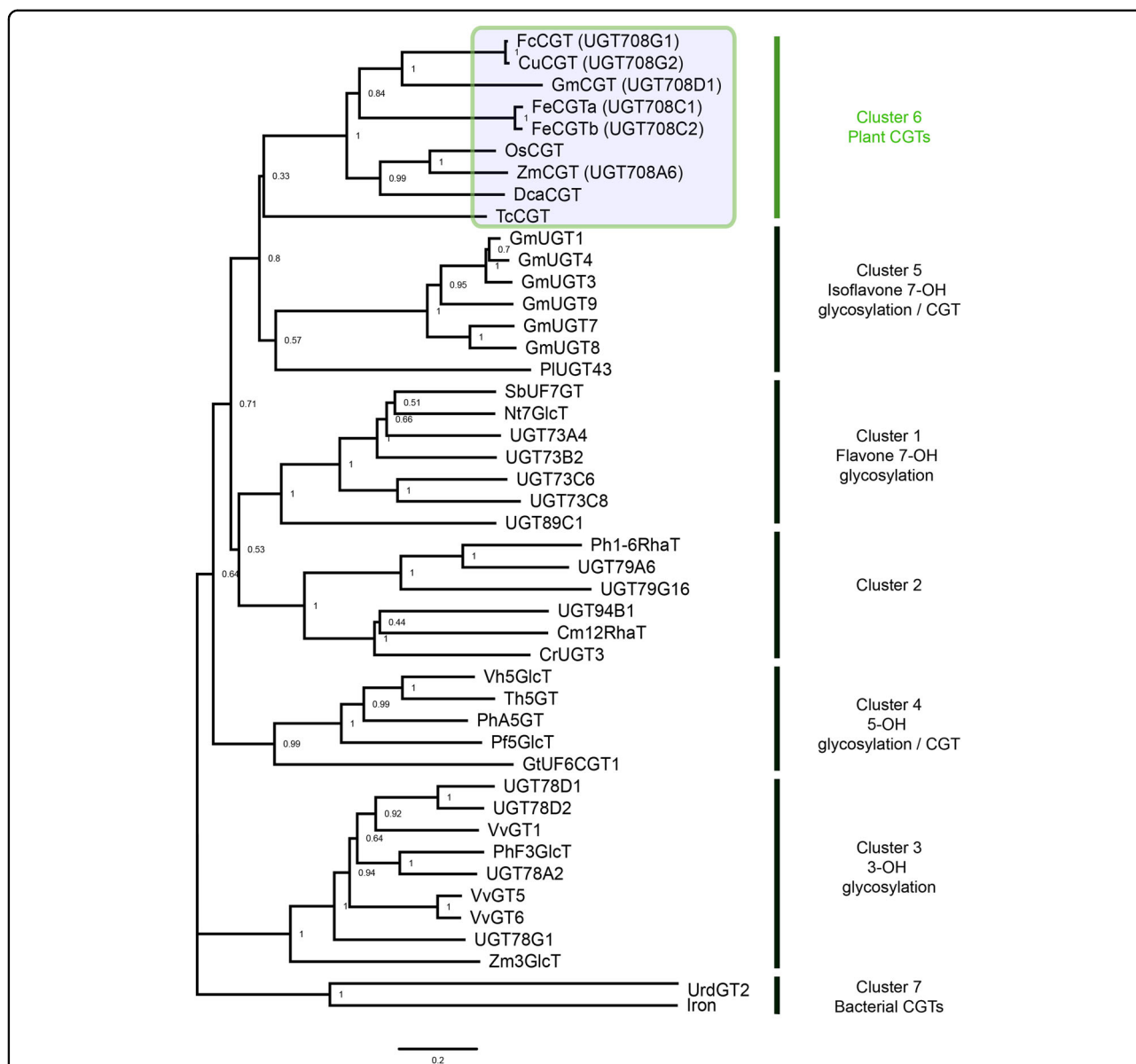


Fig. 9 Neighbor-joining tree of DcaCGT and related glycosyltransferases. Phylogenetic analysis was performed by MEGA 7.0 using the neighbor-joining method and carried out via the bootstrapping method with 1000 replicates. The UGT amino-acid sequences were aligned using ClustalW. (Accession numbers are presented in Table S5)

To assess the genetic diversity of the populations, we calculated P_i and Tajima’s D values based on the distribution of 132 haplotypes among 34 populations. According to the direction of *D. catenatum* migration²⁵, we found that the Tajima’s D value of the *D. catenatum* populations decreased from west to east, regardless of the presence or absence of ancestral populations. However, an upsurge in P_i from west to east was observed if the ancestral populations were removed (Fig. 10c, d). The diversity of eastern areas was higher than that of western areas after removing the ancestral populations (ancestral populations: Cluster_a/Cluster_abc \geq 15%). The F_{st} of the

34 populations ranged from 0~0.78766. Details of the molecular diversity, population pairwise F_{st} values, nucleotide diversity, and haplotype kinds and numbers are shown in Tables S6–8.

Discussion

In the present study, 82 *UGT* genes were identified in *D. catenatum* and clustered into 15 groups based on phylogenetic analysis. *UGT* gene products account for ~0.28% of the gene products in *D. catenatum*, <0.44% in *A. thaliana*, 0.36% in cotton, 0.4% in chickpea, and >0.23% in maize^{17,18,21,49}. In plants, 12 groups (A–G, I–M) are

factors¹⁹. Groups A, D, E, G, and L, which expanded more than others during the evolution of higher plants⁵⁰, gained the highest, second highest, and third highest numbers (21 (D), 10 (E), and 8 (A, G, L)) members, accounting for 25%, 12%, and 9.7% of the putative *UGTs* in *D. catenatum*, respectively. Members of these groups have been reported to catalyze a wide variety of substrates, such as flavonoids, terpenes, and alkaloids^{15,41}, suggesting that *D. catenatum* is rich in these kinds of metabolites. Three groups, O, P, and Q, which are found in maize but not *A. thaliana*, were also identified in *D. catenatum*. In accordance with a previous study, we concluded that group O in *D. catenatum* contained five closely related members, including four *ZOG* genes⁵⁰. Members of group O may therefore catalyze the glycosylation of cytokinins¹⁸. Group Q, a group absent in Poales and Brassicales⁴¹, was also identified during our analysis. A novel group, R, which contains members of the *UGT708* family, such as *ZmCGT*, was found in four members of *D. catenatum*. This suggests that there may be similar functional genes in *D. catenatum*.

Among the 82 genes that we identified, 78 *UGTs* were dispersed throughout the chromosomes. These *UGTs* were generally organized into clusters of 2–7 genes, and most ORFs in the clusters were oriented in the same direction. Genes in the same cluster showed high sequence similarity, reflecting their close phylogenetic relationships in the family and tandem duplication after orchid-wide genome duplication. This phenomenon also occurs in the *GT1* family of cotton²¹. The position, phase, loss, and gain of introns can serve as important indicators for understanding the evolution of a gene family within phylogenetic groups. More than half (52%) of *UGTs* lack introns, which is less than the number in maize (60%) and *Arabidopsis* (58%). Introns were abundantly present in phase 0, suggesting that their phases remained stable. We also used the MEME web server to search the conserved motifs shared among *UGT* proteins. We found a total of 10 distinct conserved motifs, among which motif 1, which encoded the *UGT* domain, was found in all the identified *UGTs*. From similar motif patterns, we concluded that differences among the groups were not significant and that the *UGTs* in *D. catenatum* are still undergoing evolution. Although most closely related members usually shared common motifs, some *UGTs*, such as *Dca003346*, *Dca009408*, and *Dca014393*, differed from the other members in their group. We speculated that the structural annotation of genes was incomplete. The specific motifs may contribute to the functional divergence of *UGTs*. Gene expression patterns can help us understand the function of these genes in different tissues. Thirty-five *UGT* genes were expressed among the nine tissues evaluated in this study. Active involvement of the above-mentioned groups in each organ confirms that these

groups have vital roles in growth hormone glycosylation. Groups D and E not only gained the most *UGT* members in *D. catenatum* but also possessed the most genes simultaneously expressed in all organs. Comparison of the day roots and night roots indicated that 12 *UGTs* were expressed either only during the day or only at night. This result suggests that some *UGTs* are expressed at specific times.

In recent years, genome-wide identification of gene families has been used to reveal pathways used to synthesize bioactive components such as geranyl and neryl glucoside in grape⁵¹ and 2-phenylethanol in peach²². In the present study, we compared the 82 *Dca UGTs* with identified *CGTs* using multiple sequence alignment and phylogenetic/evolutionary analysis. Putative genes, grouped into a clade with identified *CGTs*, were chosen as candidate genes for further verification. Based on enzyme activity, a putative di-*C*-glucosylflavone pathway in *D. catenatum* was proposed. Our results show that *DcaCGT* catalyzed both the first and second *C*-glycosylation reactions of di-*C*-glucosylflavone. This is the second enzyme possessing this catalytic ability, in addition to *FcCGT*³⁸. *DcaCGT* showed strong activity when using phloretin as the substrate and weaker activity when using 2-hydroxynaringenin as the substrate *in vitro*. When we used apigenin as a substrate, we found that a small amount of apigenin-7-*O*-glucoside remained in the reaction product. We concluded that *DcaCGT* not only catalyzed di-*C*-glucosylflavone but also processed partial active sites on *O*-glucosylflavone. However, we could not detect any *O*-glucosylflavone when we used phloretin or 2-hydroxynaringenin as a substrate. *C*-glucosylflavone was also not detected when using apigenin as a substrate. Thus, we deduced that *DcaCGT* exhibits high substrate specificity.

In our phytochemical analysis, the substrates 2-hydroxynaringenin, phloretin, and apigenin were detected only in the root, stem, and leaf, in which transcript expression was lower than that in the flowers and flower buds. The levels of the mono-*C*-glucosylflavonoid, di-*C*-glucosylflavonoid, and *O*-glucosylflavonoid products were higher in flower buds than in roots. Thus, we concluded that lower transcription led to a lower product content and that *DcaCGT* showed strong catalytic capacity *in vivo*. Comparing the amounts of the three products, we found that the accumulation of vicienin-2 and of its intermediate products vitexin and isovitexin was higher than that of nothofagin and cosmosiin in different tissues of *D. catenatum*. These results indicate that *DcaCGT* has a pivotal role in the accumulation of vicienin-2.

Flavonoids are used by organisms in response to nearly all abiotic stresses^{52,53}. *CGT*, one of the key enzymes in the flavonoid biosynthesis pathway, has continued to expand during the evolution of *D. catenatum*. Our results

show that Cluster_b/c demonstrated high differentiation resulting from ancestral and selection pressure, generating adaptable genotypes after *D. catenatum* migration. Based on the wide distribution of Cluster_c, we concluded that Cluster_c was the best genotype for acclimation. Interestingly, we found that *DcaCGT* was grouped into Cluster_c. Previous studies have reported that the accumulation of cosmoiin, which is a product of *DcaCGT* *O*-glycosylation, can strengthen the ability of *D. catenatum* to resist drought stress^{54,55}. Most wild *D. catenatum* grows on cliffs with deficient water year round²⁶, which may be the reason for the remaining *O*-glycosylation activity of *DcaCGT*. The distribution of Cluster_b led us to hypothesize that this genotype can better adapt to the environment of eastern and central China. However, whether CGTs in Cluster_b gained the same or other activities requires further study. Our results from population diversity analysis of *D. catenatum* migration show that populations in eastern China possess increased genetic variation. The ancestral Cluster_a can still be found in Yunnan, Guangdong, Zhejiang, and Hubei provinces. Yunnan and Guangdong are the ancestral region of *D. catenatum*²⁵, which is why it shows increased diversity. We concluded that human activity may lead to increased diversity in eastern areas of China. In addition, flavonoid contents in different *D. catenatum* organs indicate that multiple haplotypes may be one of the reasons for the different levels of vicenin-2 observed in different regions.

As the functions of plant CGTs have been increasingly identified, the reaction mechanisms of plant CGTs have also been gradually elucidated. Hirade et al.³⁶ showed that substituting His 20 with alanine in UGT708D1 changes *C*-glucosyltransferase activity to that of *O*-glucosyltransferase; both D85 and R292 are active sites in *C*-glucosylation. Replacing either of these sites with alanine in UGT708D1 induces the loss of *C*-glucosylation. He et al.³⁹ concluded that I94 and G284 are the two active sites for *C*-glucosylation. When I94 is replaced with glutamic acid or G284 is replaced with lysine, *TcCGT* changes from *C*- to *O*-glucosylation. Our haplotype analysis of *DcaCGT* from 34 populations indicated that the active sites of His and Asp among the 274 samples examined in this study were identical. However, the active site of Ile was replaced by Met, and the active site of Gly was replaced by Arg. Such changes in active sites used for *C*-glucosylation may be the reason for *O*-glucosyltransferase activity. Further studies are needed to delineate the CGT reactions in detail.

In summary, we isolated a novel di-*C*-/*O*-glycosyltransferase from the *D. catenatum* GT1 family and analyzed the levels of related components in different tissues of *D. catenatum*. The results of transcriptomic and metabolic profiling demonstrated that the flavonoid

distribution differed among organs. We further examined the origin and differentiation of *DcaCGT* and concluded that the remaining OGT activity may help *D. catenatum* adapt to water deficit stress. Based on previously identified active sites on UGT708D1 and *TcCGT*, we found that CGT active sites were altered in *D. catenatum*. However, we did not find distinct differences between the active sites of Cluster_b and Cluster_c. Our results show that changes in these active sites can produce OGT activity. However, further studies are needed to determine whether there are functional differences between Cluster_b and Cluster_c. Our study provides a basis for understanding the impact of environmental conditions on the biosynthesis of medically relevant compounds in *D. catenatum*. These results will lay the basis for enhancing vicenin-2 production using genetic strategies and molecular breeding in *D. catenatum*.

Conclusion

We performed a genome-wide analysis and functional verification of CGT genes in *D. catenatum*. The haplotype distribution of *DcaCGT* was assessed with 274 samples acquired from 34 populations. We isolated a novel *C*-glycosyltransferase (*DcaCGT*) from *D. catenatum* by identifying and analyzing 82 putative genes in the GT1 family. *DcaCGT* could specifically catalyze not only di-*C*-glycosylation but also *O*-glycosylation. Apart from the normal function of catalyzing 2-hydroxynaringenin and phloretin to the respective di-*C*-glycosides, *DcaCGT* also catalyzes apigenin to cosmoiin. We also established that *DcaCGT* functions expanded throughout the evolution of *D. catenatum*. The residual OGT activity may help *D. catenatum* resist drought stress. Our results reveal the biosynthetic pathways of di-*C*/*O*-glucosylflavones in medicinal orchids, and our molecular phylogenetic analysis offers insight into the evolution of the functional gene.

Materials and methods

Plant materials and chemicals

D. catenatum was obtained from Qujing, Yunnan, and authenticated by Professor Zhongjian Liu (College of Landscape Architecture, Fujian Agriculture and Forestry University). Flower buds, flowers, leaves, stems, and roots, collected from healthy 2-year-old *D. catenatum* plants, were frozen at -80°C .

2-Hydroxynaringenin, vitexin, isovitexin, phloretin, apigenin, and cosmoiin were purchased from ChemFaces (Wuhan, China). UDP-glucose was purchased from Energy Chemical (Shanghai, China). Vicenin-2 was isolated from *D. catenatum* leaves in our laboratory. Nothofagin was isolated from *Desmodium caudatum* in Haifeng Chen's laboratory (College of Pharmacy, Xiamen University).

Identification of *UGT* genes

To identify UGTs, a feature sequence of UGTs, the 44-amino-acid conserved sequence of the PSPG motif, was used as a query to perform a local BLASTP search against the *D. catenatum* genome database. The coding sequence and chromosome distribution were obtained from the same database. The molecular weight (MW) and isoelectric point (pI) of each UGT protein were calculated using the online ExPASy (http://web.expasy.org/compute_pi/) program. The domain of each UGT protein was obtained using an NCBI batch CD search (<https://www.ncbi.nlm.nih.gov/cdd/>). KofamKOALA (<https://www.genome.jp/tools/kofamkoala/>) was used to confirm the function of UDP-glycosyltransferase among the UGT candidates. The subcellular localization of each UGT protein was predicted using the online CELLO v2.5 system (<http://cello.life.nctu.edu.tw/>). The distribution of *UGT* genes and their location on chromosomes were visualized using TB tools (<https://omictools.com/tbtools-tool>).

Sequence alignment and phylogenetic analysis

The predicted amino-acid sequences of *D. catenatum* UGTs were aligned by the neighbor-joining method in ClustalX software using 10,000 bootstrap replicates. A phylogenetic tree was constructed using FigTree 1.4.3.

Sequence analysis

The exon–intron organization of *D. catenatum* UGTs was evaluated by determining intron lengths, positions, and phases in the genome. Intron phases were determined as follows: introns positioned between two triplet codons were defined as phase 0; introns positioned after the first and second base in the codon were defined as phases 1 and 2, respectively. Conserved motifs were analyzed using the MEME online program (<http://meme.nbcr.net/meme/intro.html>).

Gene expression analysis using RNA-seq

Transcriptomic data available for putative *UGT* expression in different plant organs were analyzed according to the data published by Zhang et al.²⁹. Samples of each organ (flower bud, gynandrium, labellum, sepal, root tip, root, leaf, stem, and pollen), obtained from three or more different plants, were pooled prior to sequencing. Gene expression levels are shown as FPKM values. Transcript profiles for selected *D. catenatum* UGTs were expressed as heatmaps.

Cloning of *DcaCGT* and production of recombinant protein

Total RNA of *D. catenatum* was extracted from frozen leaves using a Quick RNA Isolation Kit per the manufacturer's instructions (Huayueyang, Beijing, China). First-strand cDNA was synthesized from total RNA (568 ng)

using TransScript All-in-One First-Strand cDNA Synthesis SuperMix for PCR (TransGen Biotech, Beijing, China). PCR was performed using 1 μ L first-strand cDNA as a template and *DcaCGT*-F and *DcaCGT*-R as primers (the primer sequences are provided in Table S3). The coding sequence (CDS) of the candidate CGT gene, *DcaCGT*, was amplified using PrimerSTAR Max DNA polymerase (Takara Bio, Japan) under the following conditions: 94 °C for 5 min, 37 cycles of 94 °C for 30 sec, 55 °C for 30 sec, and 72 °C for 90 sec, followed by 72 °C for 10 min. The amplified fragment was purified from an agarose gel (Magen, China), cloned using pEAST-T5 vector (TransGen Biotech, Beijing, China), transformed in phage-resistant chemically competent *E. coli* cells (TransGen Biotech, Beijing, China), and sequenced.

The empty vector pET32a (+) (Novagen, USA) was digested with FastDigest enzymes Sca I and EcoR V (Thermo, USA). Full-length cDNA was amplified by PCR using pETF-*DcaCGT* and pETR-*DcaCGT* as primers (Table S3) and purified from an agarose gel. To obtain the recombinant plasmid, the target gene was linked with a linearized vector using an Infusion cloning system (Clontech, Japan) and transformed into *E. coli* Transetta (DE3) (TransGen Biotech, Beijing, China); 0.01 mM isopropyl β -D-1-thiogalactopyranoside was then added, and the cells were incubated for 20 h at 16 °C. The cell cultures were centrifuged at 6574 $\times g$, after which the supernatants were removed and harvested *E. coli* cells were stored at –20 °C. The *E. coli* cells were suspended in 1 \times PBS (containing 1 mM PMSF and 20 mM imidazole) and disrupted by sonication. After centrifugation at 15,000 $\times g$ for 30 min at 4 °C, the supernatants were applied to a Ni-NTA Superflow column (Qiagen, Germany) with a linear gradient of imidazole, followed by desalination-exchange buffer (pH 8.0) containing 1 mM DTT on a PD-10 Column (GE Healthcare).

UGT enzymatic activity assay

Enzymatic reactions were performed at 30 °C for 5–90 min using a 250 μ M acceptor substrate, UDP-glucoside, 1 mM DTT, 50 mM Tris-HCl (pH 8.0), and 300 ng purified protein, resulting in a total volume of 100 μ L. The reaction was terminated by adding 10 μ L 2 M HCl, followed by incubation at 60 °C for 30 min to dehydration. The protein was boiled at 100 °C for 10 min as a negative control.

Supernatants were dissolved in 100 μ L HPLC-grade methanol and analyzed via HPLC-MS/MS on an AB Sciex Triple-TOF 5600⁺ mass spectrometer coupled to a Shimadzu LC-30 AD chromatography system. Products were detected by measuring absorbance at 280 nm and 340 nm.

HPLC-MS analysis

Flower buds, flowers, leaves, stems, and roots of *D. catenatum* were ground into a powder in liquid nitrogen.

In total, 100 mg powder was weighed and transferred into a conical flask. Then, 40 mL methanol was added, and the mixture was extracted ultrasonically for 1 h at 30 °C. Extracts were concentrated using a hypobaric drying method at 60 °C. Then, 5 mL HPLC-grade methanol was used to redissolve the residues to obtain the extraction solution. All the samples were filtered through a 0.22- μ m membrane filter before analysis via HPLC-MS. 2-Hydroxynaringenin, vitexin, isovitexin, vicenin-2, phloretin, nothofagin, apigenin, and cosmosiin were confirmed by HPLC-MS analysis using authentic standards. 3',5'-Di-C-glucosylphloretin was identified by the MS² fragment. Loratadine was chosen as the internal standard. The quantification of these flavonoids was performed based on their corresponding standard curves. Each tissue type was analyzed in three biological replicates in this experiment.

HPLC-MS analysis was performed with UPLC-MS/MS (AB Sciex Triple-TOF 5600⁺ mass spectrometer coupled to a Shimadzu LC-30 AD chromatography system) to complete qualitative analysis. The detected components were sent to a Thermo Fisher UHPLC-MS/MS system consisting of an Accela ultra-high-pressure liquid chromatograph and a TSQ Quantum Ultra triple-quadrupole mass spectrometer (Thermo Fisher Scientific, San Jose, CA, USA) fitted with an ESI source for quantitative analysis. All separations were carried out with an SB-C18 column (2.1 \times 100 mm, 1.8 μ m; Agilent). The system was operated in negative ion mode at a flow rate of 0.3 mL/min using solvent A (water with 0.1% formic acid), solvent B (acetonitrile), and C (methanol). The gradient elution started from 7% B, 7% C for 0 min, followed by 9% B, 9% C in 0.3 min; 11% B, 11% C in 2.7 min; 13% B, 13% C in 3.8 min; 14% B, 14% C in 4.8 min; 18% B, 18% C in 6.5 min; 45% B, 45% C in 8.5 min; a hold for 0.7 min; and a post run time of 1.5 min for re-equilibration. An optimal MS signal response of eight analytes and IS was obtained with the following ion source parameters: spray voltage at 3500 V, capillary temperature at 320 °C, sheath gas pressure at 35 psi, and auxiliary gas pressure at 10 psi.

Haplotype analysis of *DcaCGT*

A total of 274 samples of *D. catenatum* from 34 populations and five samples of *D. huoshanense* from one population were newly resequenced using 150 paired-end cycles on a NovaSeq 6000 instrument. After quality trimming, paired-end reads were mapped to the *D. catenatum* reference genome using BWA-MEM v0.7.12-r1039 with default parameters⁵⁶. The SortSam and MarkDuplicates commands from Picard Tools v1.56 were used to mark and remove duplicates in the bam-format files. IndelRealigner and RealignerTargetCreator from GenomeAnalysisTK v3.8–1 were used to perform local realignment⁵⁷. For each sample, individual variant calling was conducted using Haplotyper and GVCFTyper from

Sentieon v201711.03⁵⁸. Coding sequences for *DcaCGT* from 274 samples were obtained using the faidx tool from SAMtools v1.9 and consensus from BCFtools v1.2⁵⁹.

The 274 *DcaCGT* sequences were aligned by ClustalX software in MEGA5. A phylogenetic tree was constructed using the *DcaCGT*-coding sequences and neighbor-joining method in MEGA5. Population genetic analysis was performed by using DnaSP 6⁶⁰. Nei's nucleotide diversity (π) and Fst were computed by Arlequin v.3.0⁶¹.

Acknowledgements

We are very thankful to Haifeng Chen's team (Xiamen University) for providing the necessary standard and Shaofeng Wu (Guangzhou University of Chinese Medicine) for providing the laboratory to accomplish our work. This project was supported by the 2018 Shaoguan City Science and Technology Plan Project: Special Project of Industry-University-Research Cooperation (no. 2018CS11919), 2019 Guangdong Province Special Fund for Science and Technology ('Big project + task list') Project: Ecological Cultivation and Sustainable Utilization of Danxia *Dendrobium officinale*, a rare Southern Medicine in Guangdong Province (no. 2019gdsjkjzjzj-zt3–2), Fundamental Research Project of Shenzhen, China (JCYJ20170817105300166), National Key Research and Development Program of China (no. 2018YFD1000401) and Key Laboratory of National Forestry and Grassland Administration for Orchid Conservation and Utilization Construction Funds (nos. 115/11899005;115/KJG18016A) awarded to Z.-J.L.

Author details

¹School of Pharmaceutical Sciences, Guangzhou University of Chinese Medicine, Guangzhou 510006, China. ²Shantou University Medical College, Shantou 515041, China. ³State Key Laboratory of Systematic and Evolutionary Botany, Institute of Botany, Chinese Academy of Sciences, Beijing 100093, China. ⁴University of Chinese Academy of Sciences, Beijing 100049, China. ⁵Shenzhen Key Laboratory for Orchid Conservation and Utilization, The National Orchid Conservation Center of China and The Orchid Conservation and Research Center of Shenzhen, Shenzhen 518114, China. ⁶Department of Pharmacy, Sun Yat-Sen Memorial Hospital, Sun Yat-Sen University, Guangzhou 510120 Guangdong, China. ⁷Shaoguan Institute of Danxia *Dendrobium officinale*, Shaoguan 512005, China. ⁸Key Laboratory of National Forestry and Grassland Administration for Orchid Conservation and Utilization, College of Landscape Architecture, Fujian Agriculture and Forestry University, Fuzhou 350002, China. ⁹Henry Fok College of Biology and Agriculture, Shaoguan University, Shaoguan 512005, China

Author contributions

Z.R. and X.J. carried out the discovery and functional identification of *DcaCGT* and wrote this manuscript. Z.J. and G.Z. analyzed the population diversity. Y.L., S.T., and J.Z. carried out the LC-MS experiments. Z.L. and Y.W. collected the samples and extracted DNA. G.W. and Z.L. are the corresponding authors and contributed significantly to the work design.

Conflict of interest

The authors declare that they have no conflict of interest.

Supplementary Information accompanies this paper at (<https://doi.org/10.1038/s41438-020-0330-4>).

Received: 6 February 2020 Revised: 20 April 2020 Accepted: 28 April 2020
Published online: 01 July 2020

References

- Ulrike, M. Flavonoid functions in plants and their interactions with other organisms. *Plants* **7**, 30 (2018).
- Casati, P. & WALBOT, V. Differential accumulation of maysin and rhamnosylisorientin in leaves of high-altitude landraces of maize after UV-B exposure. *Plant Cell Environ.* **28**, 788–799 (2005).

3. Mommer, L., Kirkegaard, J. & van Ruijven, J. Root–root interactions: towards a rhizosphere framework. *Trends Plant Sci.* **21**, 209–217 (2016).
4. Hooper, A. M. et al. Isochaftoside, a C-glycosylflavonoid from *Desmodium uncinatum* root exudate, is an allelochemical against the development of *Striga*. *Phytochemistry* **71**, 904–908 (2010).
5. Yabuya, T., Nakamura, M., Iwashina, T., Yamaguchi, M. & Takehara, T. Anthocyanin-flavone copigmentation in bluish purple flowers of Japanese garden iris (*Iris ensata* Thunb.). *Euphytica* **98**, 163–167 (1997).
6. Marrassini, C., Davicino, R., Acevedo, C., Anesini, C. & Ferraro, G. Vicenin-2, a potential anti-inflammatory constituent of *Urtica circularis*. *J. Nat. Prod.* **74**, 1503–1507 (2011).
7. Islam, M. N., Ishita, I. J., Jung, H. A. & Choi, J. S. Vicenin 2 isolated from *Artemisia capillaris* exhibited potent anti-glycation properties. *Food Chem. Toxicol.* **69**, 55–62 (2014).
8. Verspohl, E. J., Fujii, H., Homma, K. & Buchwald-Werner, S. Testing of *Perilla frutescens* extract and Vicenin 2 for their antispasmodic effect. *Phytomedicine* **20**, 427–431 (2013).
9. Lee, W., Yoon, E. K., Kim, K. M., Dong, H. P. & Bae, J. S. Anti-septic effect of vicenin-2 and scolymsoside from *Cyclopia subternata* (Honeybush) in response to HMGB1 as a late sepsis mediator in vitro and in vivo. *Can. J. Physiol. Pharm.* **93**, 709 (2015).
10. Lee, W. & Bae, J.-S. Antithrombotic and antiplatelet activities of vicenin-2. *Blood Coagul. Fibrinolysis* **26**, 628–634 (2015).
11. Luo, Y. et al. Structure identification of viceninii extracted from and the reversal of tgf- β 1-induced epithelial/mesenchymal transition in lung adenocarcinoma cells through TGF- β /Smad and PI3K/Akt/mTOR signaling pathways. *Molecules* **24**, 144 (2019).
12. Nagaprashantha, L. D. et al. Anti-cancer effects of novel flavonoid vicenin-2 as a single agent and in synergistic combination with docetaxel in prostate cancer. *Biochem. Pharmacol.* **82**, 1100–1109 (2011).
13. Li, P., Lei, K., Li, Y., He, X. & Hou, B. Identification and characterization of the first cytokinin glycosyltransferase from rice. *Rice* **12**, 19–30 (2019).
14. Stevenson, P. C., Nicolson, S. W. & Wright, G. A. Plant secondary metabolites in nectar: impacts on pollinators and ecological functions. *Funct. Ecol.* **31**, 65–75 (2017).
15. Brazier-Hicks, M., Gershater, M., Dixon, D. & Edwards, R. Substrate specificity and safener-inducibility of the plant UDP-glucose dependent family 1 glycosyltransferases super-family. *Plant Biotechnol. J.* **16**, 337–348 (2018).
16. Peng, M. et al. Differentially evolved glycosyltransferases determine natural variation of rice flavone accumulation and UV-tolerance. *Nat. Commun.* **8**, 1975 (2017).
17. Li, Y., Baldauf, S., Lim, E.-K. & Bowles, D. J. Phylogenetic analysis of the UDP-glycosyltransferase multigene family of *Arabidopsis thaliana*. *J. Biol. Chem.* **276**, 4338–4343 (2001).
18. Li, Y. et al. Genome-wide identification and phylogenetic analysis of Family-1 UDP glycosyltransferases in maize (*Zea mays*). *Planta* **239**, 1265–1279 (2014).
19. He, Y. et al. Genome-wide analysis of family-1 UDP glycosyltransferases (UGT) and identification of UGT genes for FHB resistance in wheat (*Triticum aestivum* L.). *BMC Plant Biol.* **18**, 67 (2018).
20. Mamoon Rehman, H. et al. Genome-wide analysis of family-1 UDP-glycosyltransferases in soybean confirms their abundance and varied expression during seed development. *J. Plant Physiol.* **206**, 87–97 (2016).
21. Huang, J. et al. Genome-wide analysis of the family 1 glycosyltransferases in cotton. *Mol. Genet. Genomics* **290**, 1805–1818 (2015).
22. Wu, B. et al. Genome-wide identification, expression patterns, and functional analysis of UDP glycosyltransferase family in peach (*Prunus persica* L. Batsch). *Front. Plant Sci.* **8**, 389 (2017).
23. Cheng, X. et al. Family-1 UDP glycosyltransferases in pear (*Pyrus bretschneideri*): molecular identification, phylogenomic characterization and expression profiling during stone cell formation. *Mol. Biol. Rep.* **46**, 2153–2175 (2019).
24. Zhang, Y. et al. *Dendrobium officinale* leaves as a new antioxidant source. *J. Funct. Foods* **37**, 400–415 (2017).
25. Hou, B. et al. Iteration expansion and regional evolution: phylogeography of *Dendrobium officinale* and four related taxa in southern China. *Sci. Rep.* **7**, 43525 (2017).
26. Lei, Z. et al. Transcriptome analysis reveals genes involved in flavonoid biosynthesis and accumulation in *dendrobium catenatum* from different locations. *Sci. Rep.* **8**, 6373 (2018).
27. Teixeira, dS., Jaime, A. & Ng, T. B. The medicinal and pharmaceutical importance of *Dendrobium* species. *Appl. Microbiol. Biot.* **101**, 2227–2239 (2017).
28. Yuan, Y. et al. Tissue-specific transcriptome for *Dendrobium officinale* reveals genes involved in flavonoid biosynthesis. *Genomics* **112**, 1781–1794 (2020).
29. Zhang, G. Q. et al. The *Dendrobium catenatum* Lindl. genome sequence provides insights into polysaccharide synthase, floral development and adaptive evolution. *Sci. Rep.* **6**, 1–10 (2016).
30. Zhang, X. et al. Identification and quantitative analysis of phenolic glycosides with antioxidant activity in methanolic extract of *Dendrobium catenatum* flowers and selection of quality control herb-markers. *Food Res. Int.* **123**, 732–745 (2019).
31. Wang, K. et al. *Dendrobium officinale* polysaccharide attenuates type 2 diabetes mellitus via the regulation of PI3K/Akt-mediated glycogen synthesis and glucose metabolism. *J. Funct. Foods* **40**, 261–271 (2018).
32. Yu, S. et al. Gigantol inhibits Wnt/ β -catenin signaling and exhibits anticancer activity in breast cancer cells. *BMC Complement. Altern. Med.* **18**, 59 (2018).
33. Brazier-Hicks, M. et al. The C-glycosylation of flavonoids in cereals. *J. Biol. Chem.* **284**, 17926–17934 (2009).
34. Falcone Ferreyra, M. L. et al. Identification of a bifunctional maize C- and O-glycosyltransferase. *J. Biol. Chem.* **288**, 31678–31688 (2013).
35. Nagatomo, Y. et al. Purification, molecular cloning and functional characterization of flavonoid C-glycosyltransferases from buckwheat (*Fagopyrum esculentum*) cotyledon. *Plant J.* **80**, 437–448 (2014).
36. Hirade, Y. et al. Identification and functional analysis of 2-hydroxyflavanone C-glycosyltransferase in soybean (*Glycine max*). *FEBS Lett.* **589**, 1778–1786 (2015).
37. Sasaki, N. et al. Identification of the glycosyltransferase that mediates direct flavone C-glycosylation in *Gentiana triflora*. *FEBS Lett.* **589**, 182–187 (2014).
38. Ito, T., Fujimoto, S., Suito, F., Shimosaka, M. & Taguchi, G. C-Glycosyltransferases catalyzing the formation of di-C-glycosyl flavonoids in citrus plants. *Plant J.* **91**, 187–198 (2017).
39. He, J.-B. et al. Molecular characterization and structural basis of a promiscuous C-glycosyltransferase from *Trollius chinensis*. *Angew. Chem.* **58**, 11513–11520 (2019).
40. Ng, T. B. et al. Review of research on *Dendrobium*, a prized folk medicine. *Appl. Microbiol. Biot.* **93**, 1795–1803 (2012).
41. Wilson, A. & Tian, L. Phylogenomic analysis of UDP-dependent glycosyltransferases provides insights into the evolutionary landscape of glycosylation in plant metabolism. *Plant J.* **100**, 1273–1288 (2019).
42. Zhang, G. Q. et al. The *Apostasia* genome and the evolution of orchids. *Nature* **549**, 379–383 (2017).
43. Pereira, C. A. M., Yariwake, J. H. & McCullagh, M. Distinction of the C-glycosylflavone isomer pairs orientin/isorientin and vitexin/isovitexin using HPLC-MS exact mass measurement and in-source CID. *Phytochem. Anal.* **16**, 295–301 (2005).
44. Silva, D. B. et al. Mass Spectrometry of Flavonoid Vicenin-2, Based Sunlight Barriers in *Lychnophora* species. *Sci. Rep.* **4**, 4309 (2014).
45. Stalmach, A. L., Mullen, W., Pecorari, M., Serafini, M. & Crozier, A. Bioavailability of C-linked dihydrochalcone and flavanone glucosides in humans following ingestion of unfermented and fermented rooibos teas. *J. Agric. Food Chem.* **57**, 7104–7111 (2009).
46. Roowi, S. & Crozier, A. Flavonoids in tropical citrus species. *J. Agric. Food Chem.* **59**, 12217–12225 (2011).
47. March, R. E., Lewars, E. G., Stadey, C. J., Miao, X. S. & Metcalfe, C. D. A comparison of flavonoid glycosides by electrospray tandem mass spectrometry. *Int. J. Mass Spectrom.* **248**, 61–85 (2006).
48. Wright, S. The interpretation of population structure by F-statistics with special regard to systems of mating. *Evolution* **19**, 395–420 (1965).
49. Ranu, S., Vimal, R., G. S. C. & Sara, A. Genome-wide identification and tissue-specific expression analysis of udp-glycosyltransferases genes confirm their abundance in *Cicer arietinum* (chickpea) genome. *PLoS ONE* **9**, e109715 (2014).
50. Caputi, L., Malnoy, M., Goremykin, V., Nikiforova, S. & Martens, S. A genome-wide phylogenetic reconstruction of family 1 UDP-glycosyltransferases revealed the expansion of the family during the adaptation of plants to life on land. *Plant J.* **69**, 1030–1042 (2011).
51. Bönisch, F. et al. Activity-based profiling of a physiologic aglycone library reveals sugar acceptor promiscuity of family 1 udp-glycosyltransferases from grape. *Plant Physiol.* **166**, 23–39 (2014).
52. Nakabayashi, R. & Saito, K. Integrated metabolomics for abiotic stress responses in plants. *Curr. Opin. Plant Biol.* **24**, 10–16 (2015).
53. Nan et al. *Malus sieversii*: the origin, flavonoid synthesis mechanism, and breeding of red-skinned and red-fleshed apples. *Hortic. Res.* **5**, 70 (2018).
54. Mechri, B. et al. Verbascoside and oleuropein are potential indicators of drought resistance in olive trees (*Olea europaea* L.). *Plant. Physiol. Biochem.* **141**, 407–414 (2019).

55. Hojati, M., Modarres-Sanavy, S. A. M., Ghanati, F. & Panahi, M. Hexaconazole induces antioxidant protection and apigenin-7-glucoside accumulation in *Matricaria chamomilla* plants subjected to drought stress. *J. Plant Physiol.* **168**, 782–791 (2011).
56. Li, H. & Durbin, R. Fast and accurate short read alignment with Burrows-Wheeler transform. *Bioinformatics* **25**, 1754–1760 (2009).
57. Mckenna, A. et al. The Genome Analysis Toolkit: a MapReduce framework for analyzing next-generation DNA sequencing data. *Genome Res.* **20**, 1297–1303 (2010).
58. Freed, D. N., Aldana, R., Weber, J. A. & Edwards, J. S. The Sentieon Genomics Tools - a fast and accurate solution to variant calling from next-generation sequence data. *bioRxiv* 115717 (2017).
59. Danecek, P. & McCarthy, S. A. BCFtools/csq: haplotype-aware variant consequences. *Bioinformatics* **33**, 2037–2039 (2017).
60. Librado, P. & Rozas, J. DnaSP v5: a software for comprehensive analysis of DNA polymorphism data. *Bioinformatics* **25**, 1451–1452 (2009).
61. Laurent et al. Arlequin (version 3.0): an integrated software package for population genetics data analysis. *Evol. Bioinform. Online* **1**, 47–50 (2007).